

## Supporting information:

**Table S 1:**  $D_{10}$ ,  $D_{50}$  and  $D_{90}$  values from cumulative distribution of each sample with and without metal precursor  $\text{HAuCl}_4$  respectively.

Sample	$D_{10}$	$D_{50}$	$D_{90}$
1-2 nm porous	2.47	19.3	41.0
1-2 nm porous with $\text{HAuCl}_4$	2.10	13.1	48.6
50 nm porous	1.55	9.49	43.3
50 nm porous with $\text{HAuCl}_4$	1.43	5.55	34.3
100 nm porous	1.85	12.3	48.8
100 nm porous with $\text{HAuCl}_4$	1.86	12.4	48.6
200 nm porous ground	1.73	9.97	38.3
200 nm porous with $\text{HAuCl}_4$	1.55	10.4	38.9
370 nm porous	1.49	10.4	45.3
370 nm porous with $\text{HAuCl}_4$	1.55	10.6	45.8

Particle size measurements by dynamic light scattering method reveal similar  $D_{10}$ ,  $D_{50}$  and  $D_{90}$  values for samples with and without metal salts (Table S 1). Almost no effect of metal precursor addition can be seen for the samples initially 100 nm, 200 nm and 370 nm porous glass with  $\text{HAuCl}_4$  addition. For 1-2 nm porous glass with addition of  $\text{HAuCl}_4$ , the  $D_{90}$  value is larger than for the sample without metal precursor. Contrary effects can be observed for the 50 nm sample. Following the expectation, that the hygroscopic metal salts moisturize the samples, which can result in particle agglomeration and therefore larger particles than powders without metal salts, this result is surprising. However, it should not be neglected, that the glass samples could also exhibit inherently different water content, leading to the release of water during the grinding process and therefore benefit agglomeration and different particle size distribution.

**Table S 2:** Specific surface area and total pore volume obtained from BET analyses.

sample	$A_{\text{BET}} [\text{m}^2 \text{g}^{-1}]$	Total pore volume [ $\text{ccg}^{-1}$ ]
1-2 nm porous	51	17.1
1-2 nm porous with $\text{HAuCl}_4$	71	24.1
50 nm porous	41	14.3
50 nm porous with $\text{HAuCl}_4$	25	9.56
100 nm porous	88	28.1
100 nm porous with $\text{HAuCl}_4$	43	13.1
200 nm porous	26	9.12
200 nm porous with $\text{HAuCl}_4$	27	9.33
370 nm porous	0.26	0.08
370 nm porous with $\text{HAuCl}_4$	34	12.1

BET measurements revealed different area for samples with and without precursor addition (Table S 2). For the 50 nm porous glass, the area decreased from 41 to 25  $\text{m}^2 \text{g}^{-1}$  and for the 100 nm porous glass sample the BET-surface was almost cut in half from 88 to 43  $\text{m}^2 \text{g}^{-1}$ . The effect of surface decrease could be caused by an agglomeration of glass particles facilitated by the hygroscopic tetrachloric auric acid. Interestingly, contrary results can be seen for the samples with 1-2 nm porous glass as here an increase of specific surface area could be measured from 51 to 71  $\text{m}^2 \text{g}^{-1}$ . Likewise, one could observe for the sample with 370 nm initial pore size from 0.261 to even 34  $\text{m}^2 \text{g}^{-1}$ . Regarding the sample with 200 nm initial pore size the BET surface remained equal comparing the samples round with and without  $\text{HAuCl}_4$  with 26 and 27  $\text{m}^2 \text{g}^{-1}$  respectively.

**Table S 3:** Calculations utilizing Scherrer equation comprising  $K$  (shape factor) = 0.940, the X-ray wavelength  $\lambda = 0.154$  nm and the values for full width at half maximum  $\beta$ , Bragg angle  $\Theta$  for (111)-plane in order to obtain the crystallite size  $L$ .

sample	Full width at half maximum $\beta$ [degree/rad]	Bragg angle $\Theta$ for (111)-plane [degree]	Calculated crystallite size $L$ [nm]
200 nm porous with Au	$0.293/5.11 \times 10^{-3}$	19.1	30

**Table S 4:** Average ethanol concentrations and percentual degradation rate, average CO<sub>2</sub> peak areas and percentual increase as well as volume and mass flow and catalyst mass in layer of observed catalyst system 200 nm plate B along with calculated weight hourly space velocity of the system.

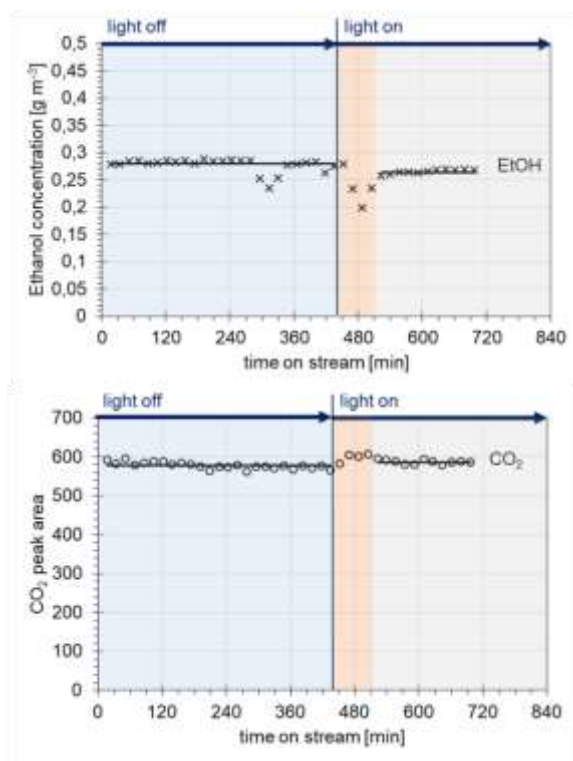
sample	average initial ethanol concentration @ 273 K [g m <sup>-3</sup> ]	average ethanol concentration @ 273 K [g m <sup>-3</sup> ]	average decrease of ethanol concentration [%]
200 nm porous with Au (plate B) 30/300	0.28	0.26	5.9

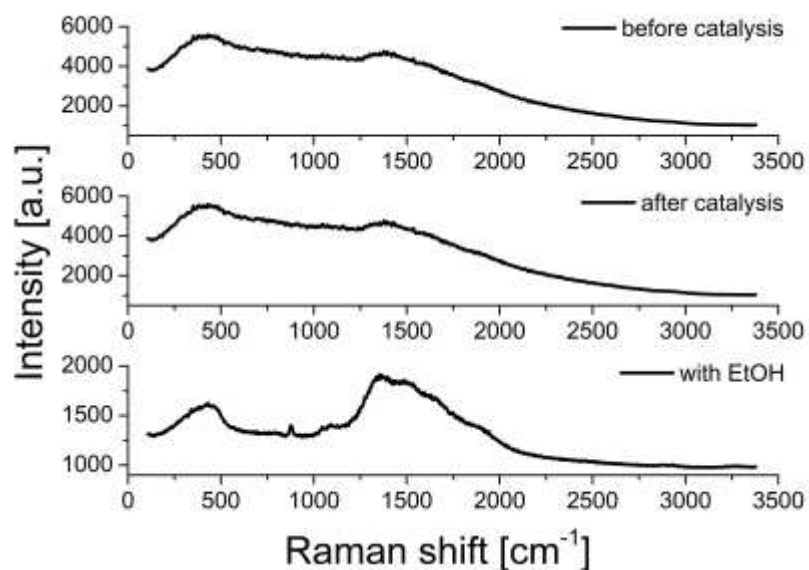
	average initial CO <sub>2</sub> peak area	average final CO <sub>2</sub> peak area	average increase of CO <sub>2</sub> peak area [%]
200 nm porous with Au (plate B) 30/300	577.41	586.35	1.5

	volume flow $\dot{V}$ [m <sup>3</sup> h <sup>-1</sup> ]	mass flow $\dot{m}$ [g h <sup>-1</sup> ]	catalyst content in layer [g]	weight hourly space velocity [h <sup>-1</sup> ]
200 nm porous with Au (plate B) 30/300	$1.98 \cdot 10^{-2}$	$5.17 \cdot 10^{-3}$	$8.70 \cdot 10^{-4}$	5.94



**Figure S 1:** Plots of ethanol concentration evolution along with evolution of CO<sub>2</sub> peak area during time on stream with light off and on.



**Figure S 2:** Raman spectra of 200 nm catalyst plate before and after catalytic process and with on purpose added model contaminant ethanol in order to verify its Raman shift.